Rules for BN-Substitution in BCN−Fullerenes. Separation of BN and C Domains

Tapas Kar,* Jayasree Pattanayak, and Steve Scheiner

Department of Chemistry and Biochemistry, Utah State University, Logan, Utah 84322-0300

Received: June 19, 2003; In Final Form: August 1, 2003

Atomic arrangements, substitution patterns, and properties of BN-doped C_{60} fullerene have been investigated using semiempirical MNDO and density functional theory (B3LYP/3-21G). The BN units prefer to stay together following "hexagon−hexagon junction", "N-site attachment", "hexagon filling" and "continuity" rules; this characteristic of atomic arrangement is independent of the compositions of BCN fullerenes. Charge redistributions after each BN substitution seem to play a guiding role for selecting the next carbon pair to be replaced by BN. The incoming BN group seeks the most highly charged carbon pairs. Up to twenty carbon pairs of C_{60} may be replaced by heteroatoms. The band gap (HOMO−LUMO gap) strongly depends on the number of BN units and their filling patterns. BN-substitution increases the electron donation capacity of fullerene.

Introduction

Hybrid BCN systems have been the subject of numerous experimental[1−4] and theoretical[5−15] studies because of their properties. They are expected to be hybrids of parent carbon and boron nitride (BN) materials. Properties intermediate between these two extremes, such as chemical inertness superior to that of diamond and a hardness greater than that of c-BN, are expected in BCN materials where CC moieties of carbon compounds have been partially substituted by BN units. It has also been predicted[15−20] that doping of h-BN into graphite structure would alter its electronic properties.

Heterofullerenes where one or more carbon atoms or pairs are substituted by boron, nitrogen, and BN pairs are gaining interest[6,21−33] as new hybrid materials. Several kinds of semiconductors can be expected from BCN materials. One is an intrinsic type of semiconductor, which can be converted to a p-type or an n-type extrinsic semiconductor by replacing C by B and N, respectively.

Methods exist by which to synthesize these hybrid materials, including chemical vapor deposition (CVD),[34−41] precursor pyrolysis,[42−46] metal-catalyzed laser ablation,[47,48] and arc discharge methods,[49,50] as well as mechanically milling mixtures of h-BN and graphite in an inert atmosphere.[51,52] A general substitution chemical reaction of carbon nanotubes (C−NTs) has been devised by which C atoms can be partially or completely substituted by B/N atoms without topological changes of the starting materials.[53−56] For example, the diameters of BCN−NTs are almost the same as those of the starting C−NTs.[55] Synthetic methods, structures, and physical and chemical properties of BCN materials have been reviewed by Itoh,[1] Kawaguchi,[2] and Terrones et al.[3,4]

Depending on synthetic methods, starting materials, temperature and pressure, different structural forms of BCN (e.g., cage structures, c-BCN, h-BCN, BCN nanotubes, thin film, nanofibers, graphitelike onion, solid solution, etc.) can be obtained. As one might expect, the ratio of B to N in these compounds is close to unity. Although different carbon concentrations[57−62] (BC_yN, $y = 0.6-7$) have been observed, the most common overall composition in all forms of BCN materials is BC_2N in both planar and nanotubular forms.

The relation between composition and properties is clearly illustrated by STM and XPS data which indicate that BC_2N film is a p-type semiconductor with a band gap of ∼2 eV, whereas a gap of half that amount has been estimated for BCN nanotubes. Watanabe and co-workers[20,63] suggest that BCN can be used as a light-emitting material. By varying the composition of the BCN compound, it is possible to tune the wavelength of the emitted light over all visible zones. Experimental evidence of such optical properties of BCN materials has been provided recently,[64−66] via blue and violet light-emitting BCN nanofibers at room temperature with adjustable optical properties. Lei et al.[67] showed that the optical band gap of BCN film deposited on glass substrates decreases monotonically as the deposition temperature increases. The dielectric constant was found to decrease with lowering growth temperature, achieving a value of 2.4[68,69] for BCN films. In summary, the properties of BCN materials strongly depend on the concentration of the constituent atoms and their arrangement.

Regarding structural details, Polo et al.[70] proposed that BC_2N films are basically a chemically mixed B−C−N ternary phase, and not a mixture of C and BN phases.[17−20,71] However, this suggestion is contradicted by other experiments[44,49,50,72,73] that point toward separate BN and C domains (C−BN−C layer arrangement) in BCN−NTs and layered materials. Random spatial distribution of B and N in C sheets, via the formation of B−C−N, B−C, and C−N bonds, has recently been reported.[71,74] A completely different atomic arrangement was proposed by Kawaguchi et al.[57] wherein the building block consists of the unit structures BCCN and BN, while BC_3N is composed of BCCCN + BNCCC.

In the present investigation, the atomic arrangements of different compositions of BCN materials are considered by successive BN substitutions. We are interested to find out "rules of BN substitution" and monitor different properties with the number of BN units in BCN systems. To avoid dangling bonds of pure carbon open nanotubes or sheet structures, C_{60} fullerene has been considered as the first case of the series. In general

* Corresponding author. E-mail: tapaskar@cc.usu.edu. Fax: 1-435-797-3390. Telephone: 1-435-797-7230.

10.1021/jp035744o CCC: $25.00
Published on Web 09/17/2003

carbon networks of different forms contain structural defects: for example, pentagons and/or heptagons embedded in hexagons. In that respect, C_{60} contains both pentagons and hexagons; hence, rules of substitution in the present case may provide useful information for other cagelike BCN systems.

The single BN-substituted C_{60} molecule $C_{58}BN$ was examined by several groups[25,32,33,75,76] using semiempirical approaches. The structure with a BN bond between two hexagons is predicted to be the most stable, compared to those having BN in a fusion position on a hexagon−pentagon border, or structures where B and N atoms are disconnected. The simplest explanation of the preference of B and N atoms to be bonded together is the formation of a dative bond between them. MNDO has also been applied[77] to diazadiborine, where two CC units are replaced by two BN pairs. This study indicated that BN-substituted benzene molecules are most stable when the BN replacements are consecutive, with alternating B and N atoms. Zhao and co-workers[78,79] extended the study of BN-substituted fullerenes by considering $C_{60-2x}(BN)_x$ and $C_{70-2x}(BN)_x$ ($x = 1-3$), using semiempirical AM1 and MNDO theories to predict their structure, stability, and electronic properties. As in small ring systems,[80,81] BN units preferred adjacent positions. Successive substitution takes place in the hexagon rings of C_{60} and C_{70}. Both AM1 and MNDO predict that substituted fullerenes have considerable stability though less so than their all-carbon analogues. Although no consistent trend in band gap was found, substituted fullerenes in general have slightly smaller gaps than pure fullerenes. It has been predicted[24] that BN−fullerenes are slightly more aromatic than C_{60}, whereas their hexaanions are significantly less aromatic than C_{60}^{-6-}.

We extended[82] the study on BN−fullerene by considering 4−7-BN-substituted C_{60} fullerenes, viz. $C_{60-2x}(BN)_x$, $x = 4-7$. The pattern of successive substitution was evaluated using density functional (B3LYP/3-21G and B3LYP/6-31G*) as well as semiempirical AM1 and MNDO. Confirming earlier findings, the first carbon pair replacement takes place at a hexagon−hexagon junction of C_{60} to form $C_{58}BN$ or 1-BN−fullerene. The next two BN units replace carbons of the same hexagon following the "hexagon-filling" rule. In the mono- and disubstituted fullerenes, one of the hexagons of C_{60} can be considered as partially BN-filled or unsaturated BN−fullerenes, while the trisubstituted fullerene is saturated or fully BN-filled. As we continue replacing CC pairs up to seven pairs, the BN units spread to the adjacent hexagons, eventually covering a pentagon. Another ruling factor of successive BN substitution is the attachment of the next BN unit to the N atom of an existing BN group. Any other structural arrangements, where BN units are not consecutive, or some of the heteroatom pairs are placed in hexagon−pentagon joints, or filling of a pentagon takes place, cause instability. The same is true with the increase of the number of intervening rings between fully BN-substituted hexagons.

Thus, up to 7-BN−fullerene, BN units of BCN fullerenes remain together, which indicates a proclivity for separate BN and C zones. In the present investigation we continue to replace −CC− units of $C_{46}(BN)_7$ (7-BN−fullerene) without any restriction.[83] Substitutions are continued until the inevitable formation of destabilizing B−B and/or N−N bonds. We hope to thus identify a maximum number for BN-substitution and to determine the limits of applicability of the aforementioned rules.

Method of Calculations

In our previous investigations[82,83] we found that trends in relative energies (E_{rel}) of different isomers of different BCN−fullerenes obtained by MNDO[84] are consistent with more accurate methods (such as B3LYP/3-21G//MNDO, B3LYP/3-21G//B3LYP/3-21G, PW91PW91//MNDO, PW91PW91/3-21G// PW91PW91/3-21G, B3LYP/6-31G*//B3LYP/3-21G, and B3LYP/6-31G*//B3LYP/6-31G*). On the basis of these findings, geometries of all systems were fully optimized without any symmetry constraints at the MNDO level. Vibrational analyses at the same level indicate that all isomers of BN-substituted C_{60} fullerenes considered in the present investigation have no imaginary frequencies, indicating a true minimum. Some of the isomers have also been treated at the B3LYP/3-21G level where the relative energies remain within 2−3 kcal/mol of those estimated by MNDO. Finally, the properties of the most stable isomers of each group were calculated using B3LYP/3-21G method. It may be worth mentioning that in this study we are less interested in the absolute magnitudes of the energies or other properties but are concentrated on their trends.

Band gaps are estimated from the energy difference between the highest occupied (HOMO) and the lowest unoccupied (LUMO) molecular orbitals. Use of the B3LYP/3-21G method and MNDO geometries seems quite reliable for determining trends in electronic properties. For example, in the case of 1−24-BN−fullerenes (CBN ball), the B3LYP/3-21G HOMO−LUMO gaps are only 4% larger than B3LYP/6-31G* values, and this ratio is independent of the number of BN units in the heterofullerenes.[83] It is worth noting that in DFT methods those orbitals are best termed as Kohn−Sham (KS) orbitals. Recently, it has been shown by Stowasser and Hoffmann[85] that the shape and symmetry of the KS orbitals are quite similar to those of the Hartree−Fock (HF) orbitals which chemists are so familiar with. The similarity between KS and HF orbitals has also been reported in several articles.[86−88] These studies indicate that Koopmann's theorem, originally based on Hartree−Fock (HF) orbitals, can be extended to KS orbitals to estimate ionization potential (IP) and electron affinity (EA). MNDO and DFT calculations are performed using the Gaussian98 program.[89]

Results and Discussion

For the sake of clarity, substitution patterns are illustrated via Schlegel diagrams which essentially "flatten" the fullerenes into a two-dimensional plane. The order of BN substitution[82] in 1−7-BN−fullerenes is illustrated by the italic red numbers in Figure 1, each of which indicates a specific BN pair. For example, the first three CC pairs to be replaced are the 22−23, 21−24, and 18−20 pairs, filling a hexagon, as indicated by the underlined black number **1**. It can be seen that the first BN substitution takes place at a hexagon−hexagon junction, and progressive substitutions spread over to the same hexagon and adjacent two hexagons (**2** and **3**). Keeping not only B and N atoms but also BN units together enhances the stability. The other crucial factor on BN substitution derived from our previous investigation is the preference of N-site attachment (N−BN) by the incoming BN group to the existing BN units. Keeping these substitution patterns in mind we proceed to replace, one by one, carbon pairs of 7-BN−fullerene by BN.

A. Substitution Sequences of BN Groups. Out of seven nitrogen atoms (N_{21}, N_{51}, N_{23}, N_{15}, N_{18}, N_{49}, and N_{48}) of 7-BN−fullerene (Figure 1), N_{21} and N_{51} are saturated (surrounded by three B atoms). Substitution at N_{23} is not favorable because replacement of $C_{47}-C_{46}$ by BN would result in unfavorable BB ($B_{46}-B_{45}$) or NN ($N_{23}-N_{46}$) bond formation. Thus, only four N atoms, namely, N_{15}, N_{18}, N_{49}, and N_{48} of 7-BN−fullerene, are active sites for next BN attachment. Relative energies (E_{rel}) of these four possible isomers *8*, *8a*, *8b* and *8c*, where the eighth

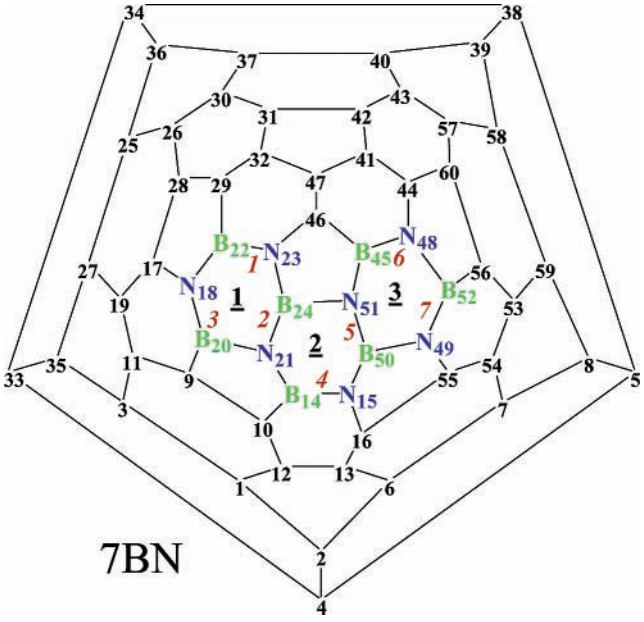

Figure 1. 1−7-BN−fullerenes. The red italic numbers indicate the order of BN substitution in sequence. The fully substituted or saturated hexagons are marked with underlined black numbers, also in sequence.

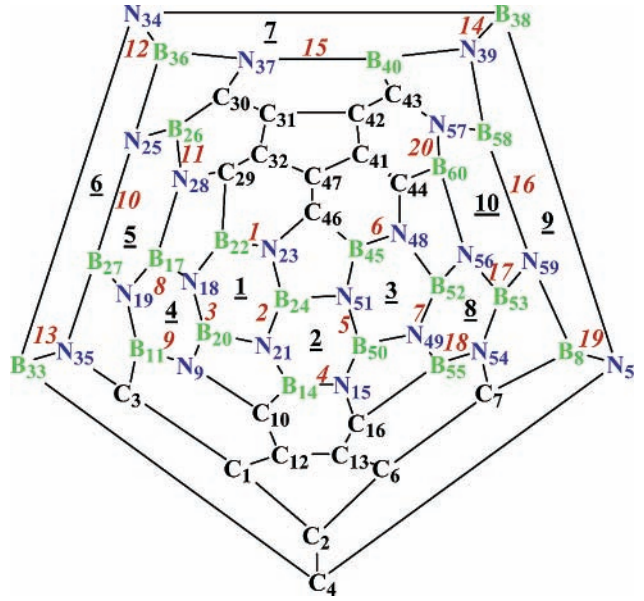

Figure 2. 8−20-BN−fullerenes. Same notations as in Figure 1.

BN unit is attached to N_{18}, N_{48}, N_{15}, and N_{49}, respectively, are reported in Table 1. It may be noted that in all these isomers, the eighth BN group is attached to the existing nitrogen atoms of 7-BN−fullerene via a N−BN link, i.e., N-site attachments. Isomer *8* is the most stable according to both MNDO and DFT methods. In fact the trend in MNDO relative energies is consistent[82,83] with more accurate methods, such as B3LYP/6-31G* using 3-21G and 6-31G* optimized geometries. In Figure 2, the position of the eighth BN group of the most stable isomer of 8-BN−fullerene is shown by the red italic number *8*. Only the positions of the BN group of the most stable isomers are shown in Figure 2, while the energetic information of various isomers of each *n*-BN−fullerenes are listed in Table 1.

We have also tested B-site attachment, i.e., where the incoming BN group replaces carbon pairs of hexagon−hexagon junctions directly bonded to existing boron atoms of 7-BN−fullerene. Similar to four active nitrogen sites, only four boron sites (B_{52}, B_{22}, B_{14}, and B_{20}) of 7-BN−fullerene are open for the eighth BN substitution via B−NB link. The relative energies of four such possible isomers (*8d*−*8g*) are reported in Table 2 along with the four N-site isomers (*8*−*8c*). It can be seen that B-site isomers are less stable by 3−6 kcal/mol, confirming the preference of "N-site" over "B-site" attachment.

TABLE 1: MNDO (DFT/3-21G) Relative Energies (E_{rel}) of Different Isomers of BCN−Fullerenes

isomers	isomers	attachment sites[a]	positions[a] B	positions[a] N	E_{rel} (kcal/mol)
8BN	*8*	N_{18}	17	19	0.00 (0.00)
	8a	N_{48}	44	41	2.64 (3.28)
	8b	N_{15}	16	13	2.85 (1.80)
	8c	N_{49}	55	54	3.31 (2.27)
9BN	*9*	N_{19}	11	9	0.00
	9a	N_{48}	44	41	8.50
	9b	N_{49}	55	54	9.39
	9c	N_{15}	16	13	9.42
	9d	N_{19}	27	25	10.55
10BN	*10*	N_{19}	27	25	0.00 (0.00)
	10a	N_{48}	44	41	2.45 (1.75)
	10b	N_{49}	55	54	3.02 (1.89)
	10c	N_{15}	16	13	5.78 (3.90)
11BN	*11*	N_{25}	26	28	0.00
	11a	N_{48}	44	41	8.92
	11b	N_{49}	55	54	9.43
	11c	N_{25}	36	34	11.01
	11d	N_{15}	16	13	11.95
12BN	*12*	N_{25}	36	34	0.00 (0.00)
	12a	N_{48}	44	41	2.35 (2.92)
	12b	N_{49}	55	54	2.84 (2.48)
	12c	N_{15}	16	13	5.44 (4.40)
13BN	*13*	N_{34}	33	35	0.00
	13a	N_{48}	44	41	8.37
	13b	N_{49}	55	54	9.53
	13c	N_{34}	38	39	10.52
	13d	N_{15}	16	13	12.16
14BN	*14*	N_{34}	38	39	0.00 (0.00)
	14a	N_{48}	44	41	2.35 (3.27)
	14b	N_{49}	55	54	2.63 (1.35)
	14c	B_{33}	2	4	4.06 (6.04)
	14d	N_{15}	16	13	5.96 (4.71)
15BN	*15*	N_{39}	40	37	0.00
	15a	N_{48}	44	41	8.43
	15b	N_{49}	55	54	8.68
	15c	N_{39}	58	59	10.96
	15d	N_{15}	16	13	11.69
	15e	B_{38}	8	5	13.05
16BN	*16*	N_{39}	58	59	0.00 (0.00)
	16a	N_{48}	44	41	1.88 (2.55)
	16b	N_{49}	55	54	2.32 (1.18)
	16c	N_{15}	16	13	5.28 (4.75)
17BN	*17*	N_{59}	53	56	0.00
	17a	N_{59}	8	5	5.07
	17b	N_{49}	55	54	14.96
	17c	N_{48}	44	41	16.07
	17d	N_{15}	16	13	17.41
	17e	N_{59}	53	54	37.02
18BN	*18*	N_{49}	55	54	0.00
	18a	N_{59}	8	5	0.00
	18b	N_{56}	60	57	4.12
	18c	N_{15}	16	13	17.31
	18d	N_{48}	44	41	17.56
19BN	*19*	N_{59}	8	5	0.00
	19a	N_{56}	60	57	0.00
	19b	N_{48}	44	41	14.02
	19c	N_{54}	7	6	14.66
	19d	N_{15}	16	13	27.55
20BN	*20*	N_{56}	60	57	0.00
	20a	N_{48}	44	41	15.24
	20b	N_{15}	16	13	27.85
	20c	N_{54}	7	6	28.51
	20d	N_5	4	2	28.68

[a] Figure 2 shows the atomic positions.

TABLE 2: Relative Energies (E_{rel}) and Mulliken Atomic Charges of 8-BN−Fullerene[a]

isomers	MNDO E_{rel} (kcal/mol)	carbon position	charge on C	carbon position	charge on C
		N-Site Attachment			
8	0.0	17	+0.16	19	−0.07
8a	2.64	44	+0.14	41	−0.05
8b	2.85	16	+0.11	13	−0.03
8c	3.31	55	+0.11	54	−0.04
		B-Site Attachment			
8d	3.29	56	−0.10	53	+0.05
8e	4.48	29	−0.09	32	+0.04
8f	6.31	10	−0.07	12	+0.02
8g	6.58	9	−0.08	11	+0.03

[a] Figure 2 shows the atomic positions.

The Mulliken charges[90,91] of selected carbon atoms of 7-BN−fullerene, involved in the eighth substitution are also summarized in Table 2. For example, in isomer *8* the $C_{17}-C_{19}$ pair of 7-BN−fullerene is substituted by the eighth BN unit. Similarly, $C_{44}-C_{41}$ pair is replaced by the heteroatoms in isomer *8a* and so on. Because of electronegativity difference among carbon, nitrogen and boron, carbon atoms attached to nitrogen (boron) atoms are positively (negatively) charged. It can be seen that the incoming B and N atoms prefer the most positively (+0.16) and negatively (−0.07) charged carbon pairs, respectively. If we consider only the isomers (*8d*−*8g*) originated from the "B-site" attachments, then B and N atoms of the most stable isomer *8d* in the group also prefer most positively and negatively charged carbons, respectively. In fact, the E_{rel} value increases as the charges decrease. Thus, it appears charge distribution may play an important role in the pattern of BN substitution.

A new substitution site (N_{19}) opens for 9-BN−fullerene in addition to the left over sites (N_{15}, N_{49}, and N_{48}) of 8-BN−fullerene. Two possible isomers (*9* and *9d*) emerge from N_{19} site. Isomer *9* is the most stable in the group because it follows the "hexagon filling" rule. So the fourth hexagon (**4** in Figure 2) is filled with BN in 9-BN−fullerene. Other isomers are less stable by more than 8.5 kcal/mol. The energy difference between the most stable isomer *9* and the second most stable isomer *9a* is more than three times the difference between *8* and *8a*. This large difference is attributed to the presence f a compltely filled hexagon (**4**) in isomer 9. Charge distribution of 8-BN−fullerene indicates that C_{11} and C_9 are the most positively (+0.14) and negatively charged (−0.11) carbons, respectively, further affirming to preference for large charge separation.

In the most stable isomer *10* of 10-BN−fullerene, the 10th BN unit replaces the carbon pair ($C_{27}-C_{25}$) attached to N_{19} of 9-BN−fullerene. It may be noted that N_{19} is the same active N site where the ninth BN unit was attached. The next stable isomer *10a* is within 2.5 kcal/mol according to MNDO. This smaller difference occurs because hexagon **5** remains unfilled in *10*. Although DFT energies are slightly different, the trends in E_{rel} are identical for both methods. The atomic charges of C_{27} (+0.16) and C_{25} (−0.07) are most positive and negative, respectively, compared to other pairs of 9-BN−fullerene involved in 10th BN substitutions. The next two substitutions take place at the new active N_{25} site: the first BN unit replaces the $C_{26}-C_{28}$ pair to complete hexagon **5** (in Figure 2) and forms 11-BN−fullerene (*11*). Again, we note the large differential that accompanies hexagon completion. The next incoming BN group spreads to the adjacent hexagon to form 12-BN−fullerene (*12*).

In fact this trend of opening active N site after each substitution and then filling the next hexagon, followed by spreading over to the next adjacent hexagon from the same active nitrogen site, continues up to 16-BN fullerenes. In this process, BN units fill three more hexagons (**5**−**7** in Figure 2). It may be noted that 15-BN−fullerene corresponds to BC_2N stoichiometry, and seven hexagons are completely filled with BN groups.

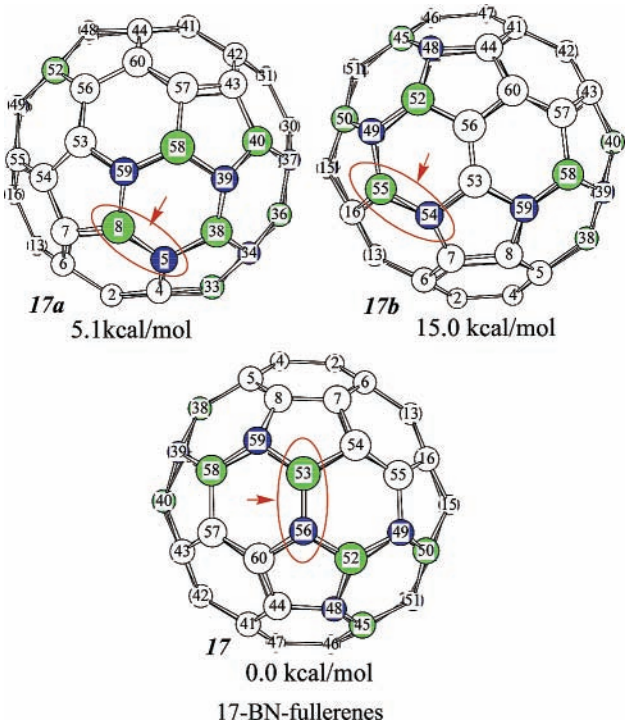

Figure 3. 3D-diagram of the isomers of 17-BN−fullerene along with relative energies. The position of the 17th BN unit is circled.

In our previous investigation,[83] we found that the "continuity rule" overshadowed the "hexagon-filling" rule for higher fullerenes where some restrictions (positions of six carbon pairs are kept fixed during the substitution process) have been imposed to reach CBN ball ($C_{12}B_{24}N_{24}$) from 7-BN−fullerene. This "continuity rule" of substitution indicates that joining existing BN chains spread over different hexagons significantly enhances the stability. In the present investigation, the 17-BN−fullerene is an example where the 17th BN unit ($B_{53}-N_{56}$) connects the existing BN chains of 16-BN−fullerene. Three-dimensional figures of *17*, *17a*, and *17b* are shown in Figure 3. Isomer *17a* is about 10.0 kcal/mol more stable than *17b* because of a filled hexagon, while *17* is 5.0 kcal/mol more stable than *17a*. The extra stability of isomer 17 may be due to conjugation. The positive and negative charges of C_{53} (+0.19) and C_{56} (−0.16) of 16-BN−fullerene are found to be maxima followed by C_8 (+0.13) and C_5 (−0.11). The CC distance (1.385 Å) of 16-BN−fullerene in the 53−56 position is found to be shortest of the five concerned CC pairs. The other distances are close to 1.400 Å. The preference of BN substitution for shorter C−C bond has already observed in previous investigations.[82]

After 17-BN−fullerene, five nitrogens (N_{49}, N_{59}, N_{56}, N_{15}, and N_{48}) are active for the next BN substitution. Of the five hexagons where the substitution positions are open, three contain one CC and two BN pairs, whereas the rest of the hexagons have one BN pair and two CC pairs. Because the stability of the isomers is enhanced by the filling of a hexagon, the former group filled one by one. Isomers *18* and *18a* are isoenergetic, whereas *18c* is less stable by 4.12 kcal/mol although all three isomers follows the same "hexagon filling" rule. The charge distributions of those carbon pairs involved in *18* ($C_{55}-C_{54}$), *18a* (C_8-C_5), and *18b* ($C_{60}-C_{57}$) indicate that C_{60} (+0.09) and

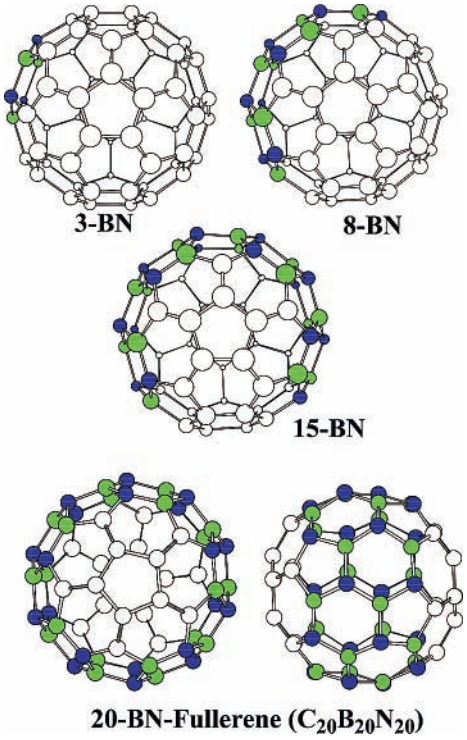

Figure 4. Progressive replacement of carbon pairs by BN units shown in 3D-diagrams of 3-, 8-, 15-, and 20-BN−fullerenes. For 20-BN−fullerene, two views from different angles are shown.

C_{57} (−0.09) are the least positively and negatively charged, respectively. The corresponding charges of C_{55}/C_{54} and C_8/C_5 are +0.13/−0.12 and +0.15/−0.12, respectively. Thus, the extra stability of *18* and *18a* may be due to higher charges of the carbon atoms compared to those of *18b*.

Three more hexagons, **8**, **9**, and **10**, are filled successively after 17-BN−fullerene by 18th, 19th, and 20th BN units as shown in Figure 2. Further substitution seems energetically not favorable because replacement of any CC pair of the remaining 10 pairs located at hexagon−hexagon junctions creates unfavorable BB or NN bonds. The other possibility is to consider hexagon−pentagon junctions for substitution. We have already seen[82] that such locations are disfavored. Furthermore, replacement of carbon pairs at the hexagon−pentagon junctions causes separation of BN units, which is not preferred by the heteroatoms. Because of these facts, further replacement of carbon pairs beyond 20-BN−fullerene (about 66.6% substitution) may destabilizes BCN−fullerene.

Three-dimensional diagrams of 3-, 8-, 15-, and 20-BN−fullerenes are shown in Figure 4 to illustrate progressive replacement of carbon pairs by BN units. For 20-BN−fullerene, two views from different angles are shown. It can be seen that the BN units start replacing carbon pairs at one hexagon−hexagon junction of the cage structure, then progressively spread in one direction covering other hexagons one by one, and finally connecting the BN units at the starting point, producing a belt of BN hexagons around the molecule. This belt leaves five carbons pairs intact on each side of the BN-band. Thus all the way from 2- to 20-BN−fullerenes, BN groups remain contiguous. It can be seen from Figure 4 that BN and C regions of BCN fullerenes, irrespective of the number of BN groups, are well separated. This observation is consistent with experimental investigations[44,49,50,72,73] in BCN systems, i.e., separate BN and C zones. Thus, our finding is in good agreement with experimental results on hybrid BCN systems.

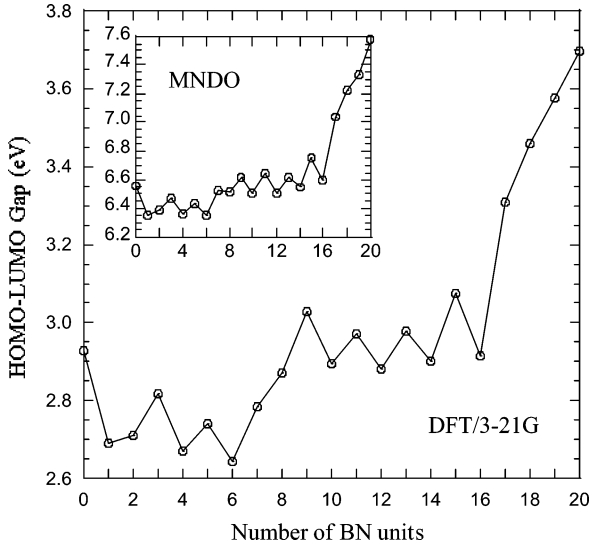

Figure 5. Variation of HOMO−LUMO gaps with the number of BN groups.

B. Geometries and Bond Indices. MNDO geometries of pure C_{60} fullerene are, in general, in good agreement[92] with more accurate theoretical methods and experimental values. The CC bond length in hexagon−hexagon (H−H) and hexagon−pentagon (H−P) junctions of fullerene are 1.40 and 1.47 Å, respectively, a difference of 0.07 Å. Similar to CC distances, different BN bond lengths at H−H and H−P junctions are predicted by MNDO theory. BN bonds in former positions (∼1.45 Å) are shorter than those located in H−P junctions by 0.04 Å. The BN bond lengths are hence less sensitive to positions than are CC bonds.

According to MNDO theory, the BN bond length in borazine ($B_3N_3H_6$) is 1.43 Å, while BN single (H_3B-NH_3) and double ($H_2B{=}NH_2$) bonds are 1.59 and 1.37 Å. Thus, the BN distances in BN−fullerenes are intermediate between single and double bonds, and slightly longer than in borazine. Because of electronegativity difference between nitrogen and boron atoms, these bonds are partially ionic. The bond indices[93−95] are close to 1.13 and 0.95 for BN bonds in H−H and H−P positions, respectively. (For perfectly covalent single and double bonds, these indices would be 1.0 and 2.0, respectively.) The corresponding bond indices are 1.54 and 1.01 for CC bonds in H−H and H−P linkages. It may be noted that the bond index is 1.5 for CC bonds of benzene.

C. HOMO—LUMO (Band) Gap and Ionization Energies. Both MNDO and DFT HOMO−LUMO gaps are plotted against the number of BN units in Figure 5. It can be seen the gap strongly depends on the methods. However, their trend is the same for both semiempirical and more accurate DFT method. In general, the MNDO band gaps in the figure inset are about 2.25 times larger than those of B3LYP/3-21G values. In a previous investigation[82] on 1−7-BN−fullerene we found that the semiempirical gap is about 2.5 times those of B3LYP/6-31G*. These ratios are almost independent of the number of BN groups.

The HOMO−LUMO (band) gap of BN−fullerene strongly depends on the number of BN units. It can be seen from Figure 5 that the gap follows a zigzag pattern up to 17-BN−fullerene and then rises sharply. A small number (up to 8) of BN doping causes lowering of the gap than the semiconducting C_{60}. From 9 to 16-BN−fullerene, the band gap is close to that of pure fullerene. After that the gap increases sharply with the increasing number of BN units, which is not surprising because pure BN systems are in general insulators.

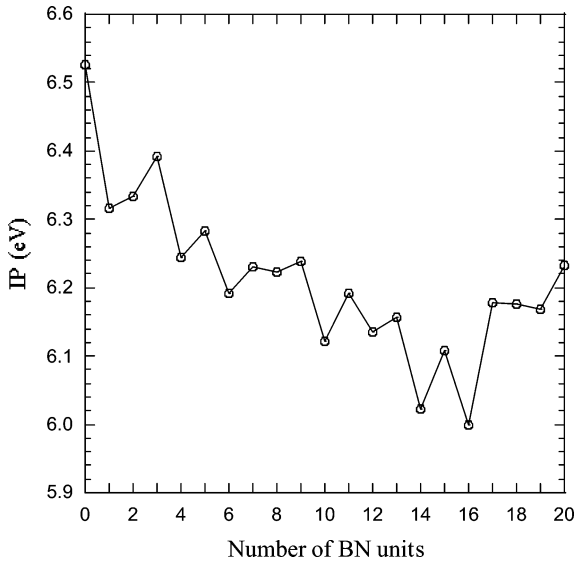

Figure 6. Variation of ionization potential (DFT/3-21G) with the number of BN units.

As reported earlier,[82] the gap of BN−fullerenes with completely BN filled hexagons (3-, 5-, 7-, 9-, 11-, 13-, and 15-BN−fullerenes) are larger than their partially filled or unsaturated (1-, 2-, 4-, 6-, 8-, 10-, 12-, 14-, and 16-BN−fullerenes) predecessor's gaps. Such a trend in the HOMO−LUMO gap is nicely followed all the way up to 17-BN−fullerene by both methods (except for the DFT gap of unsaturated 8-BN−fullerene). According to the discussed trends in gap, the MNDO value seems to correctly predict a lower gap for 8-BN−fullerene than that of 7-BN−fullerene. After 17-BN−fullerene, three hexagons are filled one by one, and thus following the saturation rule, the gap rises by each substitution.

The gap decreases in each series of filled and partially filled BN fullerenes, and the smallest value of 2.64 eV is found in 6-BN fullerene. Thus about 20% BN substitution may lower the band gap of semiconducting C_{60} by 0.28 eV (0.21 at MNDO). (It may be noted that a value of 1.8 eV has been estimated[96] experimentally for pure fullerene.) At 9-BN−fullerene the gap exceeds that of C_{60} by 0.10 eV (0.06 eV with MNDO). The gaps of the next two saturated BN−fullerenes are slightly higher than that of C_{60}, while unsaturated 12- and 14-BN−fullerenes show slightly lower gap compared to pure fullerene. The BC_2N composition (15-BN−fullerene) has a gap higher than C_{60} by 0.15 eV. The maximum change of 0.39 eV (DFT/3-21G) in HOMO−LUMO gap is found while going from 16- to 17-BN−fullerene.

Thus the gap of the entire series may be divided into three zones: 1−8-BN−fullerenes, i.e., about 27% substitution, are in "lower gap zone"; 27−53% BN−fullerene (9−16 substitutions) falls in the "parallel zone"; the rest, 53−67%, fall in the "higher gap zones". Again within the first two zones further tuning of the band gap might be possible by saturating the hexagons.

DFT/3-21G ionization potentials (IP) of the entire series of BN-substituted fullerenes are shown in Figure 6. The IP curve indicates that substituted fullerenes have smaller ionization potential relative to pure fullerene. The curve decreases in zigzag fashion all the way down to 16-BN−fullerene. This decay of IP confirms the tendency of heterofullerenes to more easily lose an electron (oxidation). The saturated BN−fullerenes show higher ionization potential compared to their unsaturated predecessors and are thus harder to oxidize. After reaching the minimum at 16-BN−fullerene (i.e., about 53% substitution), the IP curve starts moving upward, making higher BN-substituted fullerenes harder to oxidize. This reversal in not unexpected since BN systems are stable environmentally (high oxidation resistance). It is interesting to note strong similarities between the behaviors of the HOMO−LUMO gap in Figure 5 and the IP in Figure 6.

Conclusions

The possibility of tuning the properties (electronic and chemical) of fullerene has been investigated by successive BN substitutions using semiempirical and density functional methods. It has been found that BN units prefer to keep themselves connected to each other following two major rules of substitutions: "hexagon filling" and "continuity" rules. According to the former rule BN units tend to replace all three-carbon pairs of a hexagon one by one and then spread to adjacent hexagons. The "continuity" rule overshadows this rule where the incoming BN unit connects existing BN units to maintain the continuity of BN units. These two rules lead to an atomic arrangement where BN and C form separate regions in the network, consistent with several experimental investigations. This pattern of grouping heteroatoms and carbons is independent of the number of BN units.

We have also found a maximum BN substitution in carbon fullerene. Beyond that, formation of unfavorable B−B and/or N−N bonds, BN at less preferred hexagon−pentagon junctions, or separation of BN units might destabilize the hybrid fullerene.

The other factor of BN substitution is related to attachment of incoming BN units with existing BN groups. Out of two possibilities, "N-site" attachment is more favored over "B-site". The shortest CC bond in hexagon−hexagon junctions is the first target by BN unit for replacement. Charge redistribution after each substitution might play a guiding role for the incoming BN moiety: the most positively and negatively charged carbon pairs are the object for incoming heteratom pair.

The band gap (estimated from the difference of HOMO and LUMO) strongly depends on the number of BN groups and their filling pattern. For completely filled hexagons the gap is slightly higher than its unsaturated correlates. The gap decreases in a zigzag fashion, reaches a minimum at 20% of carbons substituted. Roughly three zones of band gap are identified with the number of BN units: 1 to ∼25% in lower zones (lower gap than that of semiconducting C_{60}), the parallel zone (∼25 to ∼55%), and the rest in the wide gap zone.

Similar to the band gap, the ionization potential (IP) also depends on the number of BN moieties. All heterofullerenes studied in this investigation have lower IP than that of pure carbon fullerene. The IP value also decreases in a zigzag fashion with the number of BN unit. Thus, BN substitutions make fullerene a good electron donor.

Acknowledgment. This work was supported by Grant DAAD-99-1-0206 to S.S. from the Army Research Office.

References and Notes

(1) Itoh, S. *Diamond Films Technol.* **1997**, *7*, 195−209.
(2) Kawaguchi, M. *Adv. Mater.* **1997**, *9*, 615−625.
(3) Terrones, M.; Hsu, W. K.; Hare, J. P.; Kroto, H. W.; Walton, D. R. M. *Fullerene Sci. Technol.* **1997**, *5*, 813−827.
(4) Terrones, M.; Grobert, N.; Terrones, H. *Carbon* **2002**, *40*, 1665−1684.
(5) Miyamoto, Y.; Cohen, M. L.; Louie, S. G. *Phys. Rev. B−Condens. Matter* **1995**, *52*, 14971−14975.
(6) Miyamoto, Y.; Rubio, A.; Cohen, M. L.; Louie, S. G. *Phys. Rev. B* **1994**, *50*, 4976−4979.
(7) Nozaki, H.; Itoh, S. *Phys. Rev. B* **1996**, *53*, 14161−14170.

(8) Nozaki, H.; Itoh, S. *Physica B* **1996**, *220*, 487−489.
(9) Nozaki, H.; Itoh, S. *J. Phys. Chem. Solids* **1996**, *57*, 41−49.
(10) Tateyama, Y.; Ogitsu, T.; Kusakabe, K.; Tsuneyuki, S.; Itoh, S. *Phys. Rev. B* **1997**, *55*, 10161−10164.
(11) Gal'pern, E. G.; Stankevich, I. V.; Chistyakov, A. L.; Chernozatonskii, L. A. *Russ. Chem. Bull.* **1999**, *48*, 428−432.
(12) Gal'pern, E. G.; Pinyaskin, V. V.; Stankevich, I. V.; Chernozatonskii, L. A. *J. Phys. Chem. B* **1997**, *101*, 705−709.
(13) Blase, X.; Charlier, J. C.; Devita, A.; Car, R. *Appl. Phys. Lett.* **1997**, *70*, 197−199.
(14) Blase, X.; Charlier, J. C.; De Vita, A.; Car, R. *Appl. Phys. A* **1999**, *68*, 293−300.
(15) Liu, A. Y.; Went zcovitch, M.; Cohen, M. L. *Phys. Rev. B* **1989**, *39*, 1760−1765.
(16) Rubio, A.; Corkill, J. L.; Cohen, M. L. *Phys. Rev. B* **1994**, *49*, 5081−5084.
(17) Watanabe, M. O.; Itoh, S.; Mizushima, K.; Sasaki, T. *J. Appl. Phys.* **1995**, *78*, 2880−2882.
(18) Watanabe, M. O.; Sasaki, T.; Itoh, S.; Mizushima, K. *Thin Solid Films* **1996**, *282*, 334−336.
(19) Watanabe, M. O.; Itoh, S.; Mizushima, K.; Sasaki, T. *Appl. Phys. Lett.* **1996**, *68*, 2962−2964.
(20) Watanabe, M. O.; Itoh, S.; Sasaki, T.; Mizushima, K. *Phys. Rev. Lett.* **1996**, *77*, 187−189.
(21) Guo, T.; Jin, C.; Smalley, R. E. *J. Phys. Chem.* **1991**, *95*, 4948−4950.
(22) Pradeep, T.; Vijayakrishnan, V.; Santra, A. K.; Rao, C. N. R. *J. Phys. Chem.* **1991**, *95*, 10564−10565.
(23) Piechota, J.; Byszewski, P. *Z. Phys. Chem.* **1997**, *200*, 147−155.
(24) Chen, Z.; Jiao, H.; Hirsch, A.; Thiel, W. *J. Org. Chem.* **2001**, *66*, 3380−3383.
(25) Kurita, N.; Kobayashi, K.; Kumahora, H.; Tago, K. *Fullerene Sci. Technol.* **1993**, *1*, 319−328.
(26) Bowser, J. R.; Jelski, D. A.; George, T. F. *Inorg. Chem.* **1992**, *31*, 154−156.
(27) Jensen, F.; Toftlund, H. *Chem. Phys. Lett.* **1993**, *201*, 89−96.
(28) Jensen, H.; Sorensen, G. *Surf. Coat. Technol.* **1996**, *84*, 524−527.
(29) Silaghi-Dumitrescu, I.; Haiduc, I.; Sowerby, D. B. *Inorg. Chem.* **1993**, *32*, 3755−3758.
(30) Silaghi-Dumitrescu, I.; Lara-Ochoa, F.; Bishof, P.; Haiduc, I. *J. Mol. Struct. (THEOCHEM)* **1996**, *367*, 47−54.
(31) Zhu, H.-Y.; Klein, D. J.; Seitz, W. A.; March, N. H. *Inorg. Chem.* **1995**, *34*, 1377−1383.
(32) Xia, X.; Jelski, D. A.; Bowser, J. R.; George, T. F. *J. Am. Chem. Soc* **1992**, *114*, 6493−6496.
(33) Esfarjani, K.; Ohno, K.; Kawazoe, Y. *Phys. Rev. B* **1994**, *50*, 17830−17836.
(34) Loeffler, J.; Steinbach, F.; Bill, J.; Mayer, J.; Aldinger, F. *Z. Metallkd.* **1996**, *87*, 170−174.
(35) Loiseau, A.; Willaime, F.; Demoncy, N.; Hug, G.; Pascard, H. *Phys. Rev. Lett.* **1996**, *76*, 4737−4740.
(36) Montero, I.; Galan, L. *J. Mater. Res.* **1997**, *12*, 1563−1568.
(37) Yu, J.; Wang, E. G.; Xu, G. C. *J. Mater. Res.* **1999**, *14*, 1137−1141.
(38) Popov, C.; Saito, K.; Ivanov, B.; Koga, Y.; Fujiwara, S.; Shanov, V. *Thin Solid Films* **1998**, *312*, 99−105.
(39) Polo, M. C.; Martinez, E.; Esteve, J.; Andujar, J. L. *Diamond Relat. Mater.* **1999**, *8*, 423−427.
(40) Kawaguchi, M.; Wakukawa, Y.; Nakamura, H. *J. Phys. Chem. B* **2000**, *104*, 5869−5870.
(41) Maquin, B.; Derre, A.; Labrugere, C.; Trinquecoste, M.; Chadeyron, P.; Delhaes, P. *Carbon* **2000**, *38*, 145−156.
(42) Terrones, M.; Hsu, W. K.; Terrones, H.; Zhang, J. P.; Ramos, S.; Hare, J. P.; Castillo, R.; Prasside, K.; Cheetham, A. K.; Kroto, H. W.; Walton, D. R. M. *Chem. Phys. Lett.* **1996**, *259*, 568−573.
(43) Brydson, R.; Westwood, A. V. K.; Jiang, X.; Rowen, S. J.; Collins, S.; Lu, S.; Rand, B.; Wade, K.; Coult, R. *Carbon* **1998**, *36*, 1139−1147.
(44) Kohler-Redlich, P.; Terrones, M.; Manteca-Diego, C.; Hsu, W. K.; Terrones, H.; Ruhle, M.; Kroto, H. W.; Walton, D. R. M. *Chem. Phys. Lett.* **1999**, *310*, 459−465.
(45) Sen, R.; Satishkumar, B. C.; Govindaraj, A.; Harikumar, K. R.; Raina, G.; Zhang, J.-P.; Cheetham, A. K.; Rao, C. N. R. *Chem. Phys. Lett.* **1998**, *287*, 671−676.
(46) Han, W. Q.; Cumings, J.; Zettl, A. *Appl. Phys. Lett.* **2001**, *78*, 2769−2771.
(47) Zhang, Y.; Gu, H.; Suenaga, K.; Iijima, S. *Chem. Phys. Lett.* **1997**, *279*, 264−269.
(48) Popov, C.; Ivanov, B.; Masseli, K.; Shanov, V. *Laser Phys.* **1998**, *8*, 280−284.
(49) Redlich, P.; Loeffler, J.; Ajayan, P. M.; Bill, J.; Aldinger, F.; Ruhle, M. *Chem. Phys. Lett.* **1996**, *260*, 465−470.
(50) Suenaga, K.; Willaime, F.; Loiseau, A.; Colliex, C. *Appl. Phys. A* **1999**, *68*, 301−308.
(51) Yao, B.; Chen, W. J.; Liu, L.; Ding, B. Z.; Su, W. H. *J. Appl. Phys.* **1998**, 1414−1415.
(52) Yao, B.; Liu, L.; Su, W. H. *J. Appl. Phys.* **1999**, *86*, 2464−2467.
(53) Han, W. Q.; Bando, Y.; Kurashima, K.; Sato, T. *Appl. Phys. Lett.* **1998**, *73*, 3085−3087.
(54) Han, W. Q.; Bando, Y.; Kurashima, K.; Sato, T. *Chem. Phys. Lett.* **1999**, *299*, 368−373.
(55) Golberg, D.; Bando, Y.; Han, W.; Kurashima, K.; Sato, T. *Chem. Phys. Lett.* **1999**, *308*, 337−342.
(56) Han, W. Q.; Cumings, J.; Huang, X.; Bradley, K.; Zettl, A. *Chem. Phys. Lett.* **2001**, *346*, 368−372.
(57) Kawaguchi, M.; Kawashima, T.; Nakajima, T. *Chem. Mater.* **1996**, *8*, 1197−1201.
(58) Solozhenko, V. L. *Eur. J. Solid State Inorg. Chem.* **1997**, *34*, 797−807.
(59) Solozhenko, V. L.; Andrault, D.; Fiquet, G.; Mezouar, M.; Rubie, D. C. *Appl. Phys. Lett.* **2001**, *78*, 1385−1387.
(60) Solozhenko, V. L.; Dub, S. N.; Novikov, N. V. *Diamond Relat. Mater.* **2001**, *10*, 2228−2231.
(61) Solozhenko, V. L.; Novikov, N. V. *Dopov. Nats. Akad. Nauk Ukr.* **2001**, 81−86.
(62) Komatsu, T.; Nomura, M.; Kakudate, Y.; Fujiwara, S. *J. Chem. Soc., Faraday Trans.* **1998**, *94*, 1649−1655.
(63) Chen, Y.; Barnard, J. C.; Palmer, R. E.; Watanabe, M. O.; Sasaki, T. *Phys. Rev. Lett.* **1999**, *83*, 2406−2408.
(64) Bai, X. D.; Wang, E. G.; Yu, J.; Yang, H. *Appl. Phys. Lett.* **2000**, *77*, 67−69.
(65) Zhi, C. Y.; Guo, J. D.; Bai, X. D.; Wang, E. G. *J. Appl. Phys.* **2002**, *91*, 5325−5333.
(66) Yu, J.; Ahn, J.; Yoon, S. F.; Zhang, O.; Rusli; Gan, B.; Chew, K.; Yu, M. B.; Bai, X. D.; Wang, E. G. *Appl. Phys. Lett.* **2000**, *77*, 1949−1951.
(67) Lei, M. K.; Li, Q.; Zhou, Z. F.; Bello, I.; Lee, C. S.; Lee, S. T. *Thin Solid Films* **2001**, *389*, 194−199.
(68) Sugino, T.; Etou, Y.; Tai, T.; Mori, H. *Appl. Phys. Lett.* **2002**, *80*, 649−651.
(69) Etou, Y.; Tai, T.; Sugiyama, T.; Sugino, T. *Diamond Relat. Mater.* **2002**, *11*, 985−988.
(70) Polo, M. C.; Martinez, E.; Esteve, J.; Andujar, J. L. *Diamond Relat. Mater.* **1998**, *7*, 376−379.
(71) Golberg, D.; Dorozhkin, P.; Bando, Y.; Hasegawa, M.; Dong, Z.-C. *Chem. Phys. Lett.* **2002**, *359*, 220−228.
(72) Suenaga, K.; Colliex, C.; Demoncy, N.; Loiseau, A.; Pascard, H.; Willaime, F. *Science* **1997**, *278*, 653−655.
(73) Yap, Y. K.; Yoshimura, M.; Mori, Y.; Sasaki, T. *Appl. Phys. Lett.* **2002**, *80*, 2559−2561.
(74) He, D.; Cheng, W.; Qin, J.; Yue, J.; Xie, E.; Chen, G. *Appl. Sci. Lett.* **2002**, *191*, 338−343.
(75) Chen, Z.; Ma, K.; Chen, L.; Zhao, H.; Pan, Y.; X., Z.; Tang, A.; Feng, J. *J. Mol. Struct. (THEOCHEM)* **1998**, *452*, 219−225.
(76) Piechota, J.; Byzsewski, P.; Jablonski, R.; Antonova, K. *Fullerene Sci. Technol.* **1996**, *4*, 491−507.
(77) Massey, S. T.; Zoellner, R. W. *Inorg. Chem.* **1991**, *30*, 1063−1066.
(78) Chen, Z.; Ma, K.; Zhao, H.; Pan, Y.; Zhao, X.; Tang, A.; Feng, J. *J. Mol. Struct. (THEOCHEM)* **1999**, *466*, 127−135.
(79) Chen, Z.; Ma, K.; Pan, Y.; Zhao, X.; Tang, A. *J. Mol. Struct. (THEOCHEM)* **1999**, *490*, 61−68.
(80) Kar, T.; Dalmore, D. E.; Scheiner, S. *J. Mol. Struct. (THEOCHEM)* **1997**, *392*, 65−74.
(81) Kar, T.; Cuma, M.; Scheiner, S. *J. Mol. Struct. (THEOCHEM)* **2000**, *556*, 275−281.
(82) Pattanayak, J.; Kar, T.; Scheiner, S. *J. Phys. Chem A* **2001**, *105*, 8376−8384.
(83) Pattanayak, J.; Kar, T.; Scheiner, S. *J. Phys. Chem A* **2002**, *106*, 2970−2978.
(84) Dewar, M. J. S.; Thiel, W. *J. Am. Chem. Soc.* **1977**, *99*, 4899−4907.
(85) Stowasser, R.; Hoffmann, R. *J. Am. Chem. Soc.* **1999**, *121*, 3414−3420.
(86) Yang, W.; Mortier, W. J. *J. Am. Chem. Soc.* **1986**, *108*, 5708.
(87) Hoffmann, R. *J. Mol. Struct. (THEOCHEM)* **1998**, *424*, 1−6.
(88) Kar, T.; Angyan, J. G.; Sannigrahi, A. B. *J. Phys. Chem.* **2000**, *104*, 9953−9963.
(89) Frisch, M. J.; Trucks; H. B. Schlegel, G. W.; Scuseria, G. E.; Robb, M. A.; Cheeseman, J. R.; Zakrzewski, V. G.; Montgomery, J., J. A.; Stratmann, R. E.; Burant, J. C.; Dapprich, S.; Millam, J. M.; Daniels, A. D.; Kudin, K. N.; Strain, M. C.; Farkas, O.; Tomasi, J.; Barone, V.; Cossi, M.; Cammi, R.; Mennucci, B.; Pomelli, C.; Adamo, C.; Clifford, S.; Ochterski, J.; Petersson, G. A.; Ayala, P. Y.; Cui, Q.; Morokuma, K.; Malick, D. K.; Rabuck, A. D.; Raghavachari, K.; Foresman, J. B.; Cioslowski, J.;

Ortiz, J. V.; Baboul, A. G.; Stefanov, B. B.; Liu, G.; Liashenko, A.; Piskorz, P.; Komaromi, I.; Gomperts, R.; Martin, R. L.; Fox, D. J.; Keith, T.; Al-Laham, M. A.; Peng, C. Y.; Nanayakkara, A.; Gonzalez, C.; Challacombe, M.; Gill, P. M. W.; Johnson, B.; Chen, W.; Wong, M. W.; Andres, J. L.; Gonzalez, C.; Head-Gordon, M.; Replogle, E. S.; Pople, J. A. 1998, Gaussian, Inc., Pittsburgh, PA, 1998.

(90) Mulliken, R. S. *J. Chem. Phys.* **1955**, *23*, 1833−1840.

(91) Mulliken, R. S. *J. Chem. Phys.* **1955**, *23*, 1841−1846.

(92) Cioslowski, J. *Electronic Structure Calculations on Fullerenes and their Derivatives*; Oxford University Press: New York, 1995.

(93) Kar, T. *J. Mol. Struct (THEOCHEM)* **1993**, *283*, 313−315.

(94) Sannigrahi, A. B.; Kar, T. *Chem. Phys. Lett.* **1990**, *173*, 569−572.

(95) Sannigrahi, A. B. *Adv. Quantum Chem.* **1991**, *23*, 301−351.

(96) Dresselhaus, M. S.; Dresselhaus, G.; Eklunf, P. C. *Science of Fullerenes and Carbon Nanotubes*; Academic Press: New York, 1996.